Research Article

Pulmonary Circulation

The impact of ambrisentan and tadalafil upfront combination therapy on cardiac function in scleroderma associated pulmonary arterial hypertension patients: cardiac magnetic resonance feature tracking study

Takahiro Sato[1], Bharath Ambale-Venkatesh[2], Joao A.C. Lima[3], Stefan L. Zimmerman[2], Ryan J. Tedford[3], Tomoki Fujii[3], Olivia L. Hulme[1], Erica H. Pullins[1], Celia P. Corona-Villalobos[2], Roham T. Zamanian[4], Omar A. Minai[5], Reda E. Girgis[6], Kelly Chin[7], Rubina Khair[1], Rachel L. Damico[1], Todd M. Kolb[1], Stephen C. Mathai[1] and Paul M. Hassoun[1]

[1]Division of Pulmonary and Critical Care Medicine, Department of Medicine, Johns Hopkins University School of Medicine, Baltimore, MD, USA; [2]Department of Radiology and Radiological Science, Johns Hopkins University School of Medicine, Baltimore, MD, USA; [3]Division of Cardiology, Department of Medicine, Johns Hopkins University School of Medicine, Baltimore, MD, USA; [4]Division of Pulmonary & Critical Care Medicine, Stanford University School of Medicine, Stanford, CA, USA; [5]Division of Pulmonary and Critical Care Medicine, The Cleveland Clinic, Cleveland, OH, USA; [6]Division of Pulmonary Medicine, Spectrum Health/Michigan State University, Grand Rapids, MI, USA; [7]Division of Pulmonary and Critical Care Medicine, University of Texas Southwestern Medical Center, Dallas, TX, USA

Abstract

The aim of this study was to evaluate the effect of upfront combination therapy with ambrisentan and tadalafil on left ventricular (LV) and right ventricular (RV) function in patients with systemic sclerosis-associated pulmonary arterial hypertension (SSc-PAH). LV and RV peak longitudinal and circumferential strain and strain rate (SR), which consisted of peak systolic SR (SRs), peak early diastolic SR (SRe), and peak atrial-diastolic SR (SRa) were analyzed using cardiac magnetic resonance imaging (CMRI) data from the recently published ATPAHSS-O trial (ambrisentan and tadalafil upfront combination therapy in SSc-PAH). Twenty-one patients completed the study protocol. Measures of RV systolic function (RV free wall [RVFW] peak longitudinal strain [pLS], RVFW peak longitudinal SRs [pLSRs]) and RV diastolic function (RVFW peak longitudinal SRa [pLSRa], RVFW peak circumferential SRe) were improved after treatment. LV systolic function (LV peak global longitudinal strain [pGLS]) and diastolic function (LV peak global longitudinal SRe [pGLSRe]) were also significantly improved at follow-up. Increased 6-min walk distance was significantly correlated with RVFW pLS and pLSRs, while the decrease in N-terminal pro-brain natriuretic peptide was correlated with LV pGLS. Increased cardiac index was associated with improved LV pGLSRe, and reduction in mean right atrial pressure was correlated with improved RVFW pLS and pLSRa. Combination therapy was associated with a significant improvement in both RV and LV function as assessed by CMR-derived strain and SR. Importantly, the improvement in RV and LV strain and SR correlated with improvements in known prognostic markers of PAH. (Approved by clinicaltrials.gov [NCT01042158] before patient recruitment.)

Keywords

pulmonary arterial hypertension, cardiac magnetic resonance imaging, combination therapy, systemic sclerosis, strain and strain rate

Date received: 27 May 2017; accepted: 8 November 2017

Pulmonary Circulation 2011; 8(1) 1–11
DOI: 10.1177/2045893217748307

Introduction

Pulmonary arterial hypertension (PAH) is one of the leading causes of mortality and morbidity in patients with systemic

Corresponding author:
Paul M. Hassoun, Division of Pulmonary and Critical Care Medicine, 1830 E. Monument Street, Baltimore, MD 21205, USA.
Email: phassou1@jhmi.edu

sclerosis (SSc).[1] Large clinical trials have consistently demonstrated that patients with SSc-associated PAH (SSc-PAH) remain less responsive to therapy compared to patients with idiopathic PAH (IPAH).[2,3]

Right ventricular (RV) dysfunction is the single most important determinant of outcome in patients with PAH,[4] including SSc-PAH.[5,6] Therefore, appropriate assessment of RV function appears crucial in evaluating the prognosis of SSc-PAH patients. While there is no consensus on the best assessment of RV function in patients with PAH, recent studies of non-invasive measures have demonstrated prognostic value, including echocardiography derived tricuspid annular plane systolic excursion (TAPSE)[7] and cardiac magnetic resonance (CMR)-based assessment of RV ejection fraction (EF).[8] Recognizing that the RV shares with the left ventricle (LV) muscle fibers and the interventricular septum (IVS), and that both are contained in the pericardial sac, changes in RV morphology and/or function affect the LV through ventricular interdependence.[9] Recently, a few studies demonstrated that impaired LV function is associated with clinical worsening and mortality in PAH patients.[10–12]

The recent ATPAHSS-O study demonstrated that upfront combination therapy with ambrisentan and tadalafil significantly improved symptoms (World Health Organization [WHO] functional class [FC]), 6-min walk distance (6MWD), hemodynamics, RVEF, and TAPSE after 36 weeks of therapy.[13] RV and LV strain and strain rate (SR), which are obtained from CMR and calculated from multimodality tissue tracking (MTT), have emerged as powerful tools to accurately quantify myocardial mechanics, including various directions and segments.[14] RV strain analysis has been shown to be a useful tool in assessing disease severity[15] and prognosis[16] in patients with PAH, but has not yet been used to measure PAH specific therapeutic response. In addition, LV strain analysis is a promising tool for the accurate assessment of LV function before overt systolic dysfunction develops.[17] Therefore, LV strain may be an ideal tool to assess subclinical LV dysfunction in patients with PAH where LVEF is typically within normal limits.

Therefore, the aim of this study was twofold. We first sought to assess the effect of ambrisentan and tadalafil upfront combination therapy on strain and SR of both ventricles in SSc-PAH patients enrolled in the ATPAHSS-O study.[13] Second, we examined the relationship between changes in CMR strain and SR and clinical and hemodynamic parameters before and after combination therapy. We hypothesized that CMR-based measures of RV and LV strain and SR would provide novel, non-invasive prognostic information in patients receiving medical PAH therapy.

Methods

We studied patients with SSc-PAH enrolled in the ATPAHS-O clinical trial. This multicentric, open-label, 36-week clinical trial of ambrisentan and tadalafil combination therapy in patients with SSc-PAH was approved by the institutional review boards at each center (Johns Hopkins University, Stanford University, University of Texas Southwestern Medical Center, and Cleveland Clinic) and it was registered at clinicaltrials.gov (NCT01042158) before patient recruitment.

Individuals aged older than 18 years who fulfilled the criteria for SSc and had PAH confirmed by right heart catheterization (RHC) with WHO FC II or III symptoms, but who had not yet received PAH-specific therapy, were enrolled after informed consent was obtained.

Before initiation of study drugs, participants underwent baseline clinical assessment, including WHO FC, 6MWD, and baseline blood testing (including N-terminal pro-brain natriuretic peptide [NT-proBNP]). CMR imaging (CMRI) and RHC were performed at baseline and after 36 weeks of treatment. At each time point, CMRI and RHC were performed within 24 h of each other.

CMRI

Volumetric cine images were acquired and analyzed to assess RV mass and function. All CMRI studies were read at Johns Hopkins University by two investigators (CPC-V and SLZ) blinded to the individual and study timing. Segmented fast gradient echo (FGRE) cine imaging was used at Johns Hopkins University (3-T Trio, Siemens Healthcare, Erlangen, Germany; $n = 8$). Steady-state free-precession (SSFP) cine imaging was used at University of Texas Southwestern Medical Center (1.5-T Intera, Phillips, Amsterdam, Netherlands, $n = 10$), Stanford University (1.5-T Signa HDxt, GE Healthcare, Little Chalfont, UK, $n = 6$), and Cleveland Clinic (1.5-T Achieva, Phillips, Amsterdam, Netherlands, $n = 1$). A short-axis stack of 8–10 slices covering the entire ventricle, and two long-axis cine loops of two- and four-chamber views were obtained. Typical imaging parameters were: slice thickness = 6–8 mm; field of view = 32–36 cm; minimum TR/TE; pixel size = 1.4×1.4 mm, with temporal resolution < 50 msec.

Tissue tracking CMR

We used off-line semi-automated multimodality tissue-tracking software version 6.0 (Toshiba, Tokyo, Japan) to analyze the RV and LV strain and SR. Multimodality tissue-tracking reads characteristic pixel patterns in each 10×10 mm area as template blocks from the reference image. A search is performed in the next frame to find image blocks that best match the template block, such that the best match minimizes the mean squared error of the image pixel intensity (between current image block and template block). This procedure was repeated for all pixels in each image and for each frame to track moving pixels through the whole cardiac cycle.[14,18,19] After the upload of the CMR image, the brightness was optimized to ensure optimal endocardial/blood pool discrimination.

The endocardial border of the ventricle was then manually traced on the end-diastolic frame and the software automatically propagated the endocardial borders through the cardiac cycle. Adjustment of tracked border was performed, as necessary, after visual assessment during cine loop playback by the reader.

RV free wall (RVFW) peak longitudinal strain (pLS) and SR data were directly obtained from cine images in the four-chamber view (Fig. 1a). RVFW peak circumferential strain (pCS) and SR were obtained at mid-cavity level from short-axis images (Fig. 1b). LV peak global longitudinal strain (pGLS) and SR were calculated by averaging all of the strain values obtained in long-axis two- and four-chamber images (Fig. 1c and 1d). LV pLS and SR assessed from the four-chamber image were each divided into six segments: base IVS; mid IVS; apex IVS; base lateral wall (LW); mid LW; and apex LW. LV IVS and LW pLS and SR were calculated by averaging over each of the three septal and lateral wall segments, respectively (Fig. 1e). LV pCS and SR were assessed at the short-axis mid-cavity level (same as RV circumferential analysis image) each divided into six segments: septal; anteroseptal; anterior; lateral; posterior; and inferior. LV pCS and SR were calculated by averaging all six segments. LV IVS pCS and SR were calculated by averaging septal and anteroseptal segments, and LV free wall (FW) pCS and SR were calculated by averaging anterior, lateral, posterior, and inferior segments.

A negative strain value indicates shortening with respect to the reference configuration at end-diastole defined as the peak of R wave on surface ECG. Ventricular peak systolic strain was identified from the strain curve (Fig. 2a). Peak systolic strain rate (SRs), peak early diastolic strain rate (SRe), and peak atrial-diastolic strain rate (SRa) were obtained from the SR curve (Fig. 2b).

Statistical analysis

Continuous variables are presented as median and interquartile range (IQR) considering the relatively small sample size and the fact that 26 out of 96 strain parameters were in non-normal distribution as confirmed by the Shapiro–Wilk test. Categorical variables are presented as percentages. Comparisons before and after treatment were performed using Wilcoxon signed-rank test.

Correlations of differences between before and after strain and SR parameters with other parameters were assessed using Spearman's rho test. All statistical analyses were performed using JMP® Version 11 (SAS Institute, Inc., Cary, NC, USA), and P values < 0.05 were considered statistically significant.

The intra-observer agreement for measurements was assessed by comparing the measurements of repeated analysis in ten randomly chosen individuals (TS). The inter-observer agreement was assessed using the same patients

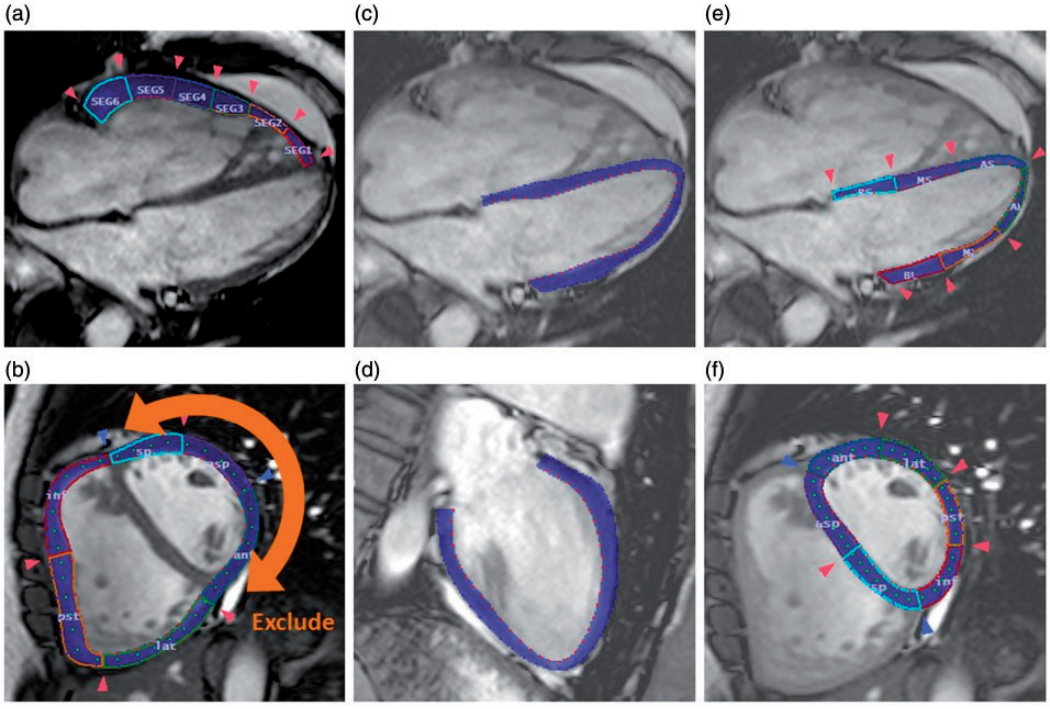

Fig. 1. Representative images of peak SRs and peak SR analysis. RV and LV measurements by tissue-tracking CMR in a patient with scleroderma-associated PAH. (a) RV peak longitudinal strain and SR measurement in four-chamber view. (b) RV peak circumferential strain and SR measurement in the short-axis view at the mid-level RVFW and LVFW were traced as a whole. After that we confirmed six segments then we excluded three of the LVFW segments. (c, d) LV peak global longitudinal strain in the two- and four-chamber views at the end of LV systole. (e) LV pLS and SR analysis in four-chamber view. (F) LV peak circumferential strain and SR in the short-axis view at the mid-level.

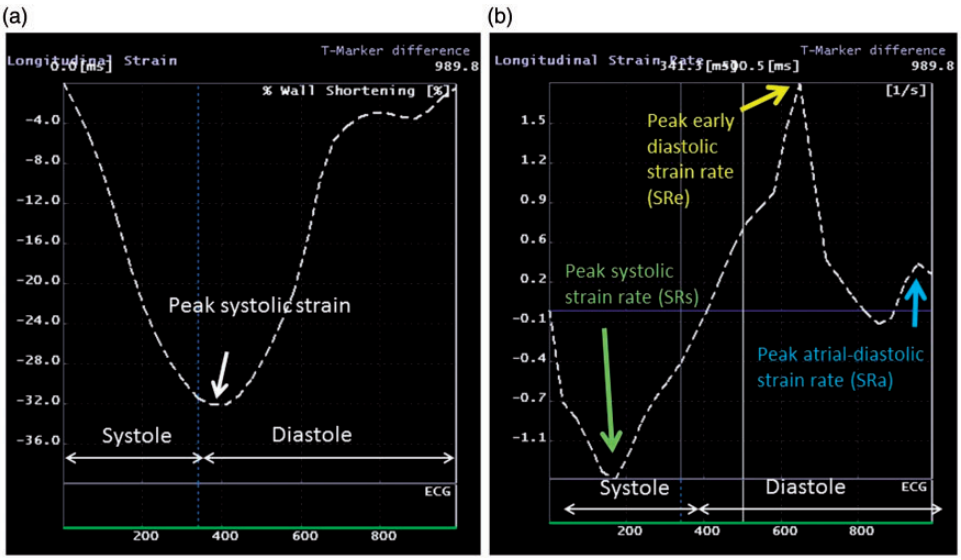

Fig. 2. Representative curves of strain and SR (e.g. RV longitudinal strain and SR analysis). Peak systolic strain was identified from the strain curve (a). Peak SRs, peak SRe, and peak SRa were also analyzed from the SR curve (b).

by comparing the results measured by TS and those obtained by an experienced radiologist (TF). The radiologist was not aware of the CMR measurements of the first examiner. Bland–Altman analysis between the two measurements was used to assess reproducibility.

Results

Twenty-five treatment-naïve individuals were enrolled. One individual was withdrawn from the study due to a complicated viral infection, one individual had no baseline CMRI assessment, and two individuals had inadequate follow-up images (motion artifact and external wire artifact) and were excluded. Therefore, the final study cohort consisted of 21 patients with pre- and post-treatment MRI exams. Among these, three patients did not have baseline two-chamber view images obtained. Thus, we analyzed 21 pairs of RV longitudinal, RV circumferential, LV four-chamber view, and LV circumferential images and 18 pairs of LV two-chamber view strain images.

There were several cases for which SR data could not be obtained due to SRa–SRe fusion and undetectable SRa. Therefore, RVFW peak longitudinal SRa (pLSRa), RVFW peak circumferential SRa (pCSRa), LV IVS pLSRa, LV peak circumferential SRe (pCSRe), and LV pCSRa were limited to 20, 18, 17, 20, and 19 studies paired at baseline and 36 weeks, respectively.

At week 36, 19 treated SSc-PAH patients were receiving ambrisentan 10 mg and tadalafil 40 mg once daily, one patient was on ambrisentan 5 mg and tadalafil 20 mg, and one patient on tadalafil 40 mg alone.[13]

Patient demographics are shown in Table 1. Patients were mostly women and white, with a median age of 63 years, and had limited SSc. They had moderate functional impairment (WHO FC II/III distribution of 8/13) with a median 6MWD of 390 m at baseline.

Table 2 shows the change in WHO-FC, 6MWD, NT-proBNP, hemodynamics parameters, and CMR parameters after treatment. As shown, significant improvement was seen in 6MWD and hemodynamics (mean pulmonary arterial pressure [Mpap], pulmonary vascular resistance [PVR], cardiac index [CI]). Additionally, RVEF, LVEDV, and LVESV were significantly increased and RVESV was significantly decreased.

Impact of combination therapy on RV and LV strain and SR

Changes in RV strain and SR from baseline to 36 weeks are shown in Table 3. Compared to baseline values, measures of RV systolic (RVFW pLS and peak longitudinal SRs [pLSRs]) and RV diastolic (RVWF pLSRa and pCSRe) were significantly increased after treatment.

Changes in LV strain and SR from baseline to 36 weeks are shown in Table 4. Combination therapy was associated with significant improvements in LV systolic function, reflected by increased LV pGLS. LV peak global longitudinal SRe (pGLSRe) was increased, whereas LV peak global longitudinal SRa (pGLSRa) was decreased. In contrast, there were no significant changes in the LV circumferential strain and SR.

Table 5 shows LV longitudinal and circumferential septal and non-septal strain and SR from baseline to 36 weeks. Compared to baseline values, LV IVS pLS, LV IVS peak longitudinal SRe (pLSRe), LV LW pLSRe, LV LW pLSRa, and LV IVS pCRSe were all significantly improved.

Relationship of change in clinical and hemodynamic parameters to change in RV and LV EF, strain, and SR

The changes in LVEF and RVEF had no significant correlation with the changes in 6MWD, NT-proBNP, and

Table 1. Baseline demographics and characteristics.

Patients (n)	21
Age, years (range)	63 (53–68)
Female, n (%)	19 (90.5)
Race, n (%)	
White	19 (90.5)
Black	1 (4.8)
Other	1 (4.8)
Limited scleroderma, n (%)	19 (90.5)
Autoantibodies, n (%)	
ACA positive	1 (4.8)
Scl-70 positive	7 (33.3)
ANA titer > 160	16 (76.2)
NT-proBNP, pg/mL	426 (140–1517)
Creatinine, mg/dL	0.9 (0.8–1.1)
eGFR < 60 mL/min/1.73 m^2, n (%)	8 (38.1)
Serum sodium, mEq/L	138 (137–140)
Hemoglobin, g/dL	12.4 (10.6–13.6)
Systemic hypertension, n (%)	9 (42.9)
Diabetes mellitus, n (%)	2 (9.5)
NYHA functional class, n (%)*	
I	0
II	8 (38.1)
III	13 (61.9)
IV	0
6MWD, m	390 (260–438)
Calcium channel blocker, n (%)	4 (19)
Diuretic therapy, n (%)	18 (85.7)
Digoxin, n (%)	1 (4.8)

Data on ACAs were available for 12 individuals; data on Scl-70 antibodies were available for 17 individuals; data on ANA were available for 18 individuals. All data reported as median (IQR) (n = 21 for each parameter).
ACA, anti-centromere antibody; ANA, antinuclear antibody; NT-proBNP, N Terminal brain natriuretic peptide; eGFR, estimated glomerular filtration rate; NYHA, New York Heart Association; 6MWD, 6-min walk distance.

hemodynamics (CI, right atrial pressure [RAP], mPAP, PVR, stroke volume [SV] index) .

Figure 3 shows the correlations between changes in 6MWD, NT-proBNP, hemodynamic parameters and RVEF, and CMR-derived strain and SR from baseline to 36 weeks. After treatment, 6MWD improvements were significantly correlated with improvement in RV systolic function as reflected by RVFW pLS ($\rho = -0.63$, $P < 0.005$) and RVFW pLSRs ($\rho = -0.5$, $P < 0.05$). NT pro-BNP levels were significantly correlated with improvement in LV systolic function as reflected by LV pGLS ($\rho = 0.5$, $P < 0.05$). Improvements with CI were significantly correlated with improvement in LV diastolic function (as reflected by LV pGLSRe [$\rho = 0.63$, $P < 0.005$]). Reductions in mean RAP (mRAP) were significantly correlated with improvement in RV systolic function (as reflected by RVFW pLS [$\rho = 0.5$, $P < 0.05$]] and RV diastolic function (as reflected by RVFW pLSRa ($\rho = 0.5$, $P < 0.05$)]. Reductions in mPAP were significantly correlated with improvement in RV diastolic function (as reflected by RVFW pLSRa [$\rho = -0.71$, $p < 0.0005$]). Improvements in PVR were significantly correlated with improvement in RV diastolic function (as reflected by RVFW pLSRa [$\rho = -0.54$, $P < 0.05$]), LV systolic function (as reflected by LV pCS [$\rho = -0.44$, $P < 0.05$]). SV index increases were significantly correlated with improvement in RV systolic function (as reflected by RVFW peak circumferential SRs [pCSRs] [$\rho = -0.47$, $P < 0.05$]), LV systolic function (reflected by LV pCS [$\rho = -0.55$, $P < 0.05$] and LV pCSRs [$\rho = -0.56$, $P < 0.05$]). Finally, RVEF changes were significantly correlated with improvement in LV systolic function (as reflected by LV pGLS [$\rho = -0.52$, $P < 0.05$]), LV diastolic function (as reflected by LV pGLSRe [$\rho = 0.59$, $P < 0.001$]), and RV systolic function (as reflected by RV pCS [$\rho = -0.48$, $P < 0.05$]).

Reproducibility

Limits of agreement with confidence intervals, as assessed by Bland–Altman analysis for intra-observer variability of strain and SR indices, are shown in Supplemental Table 1. Regarding the inter-observer variability, limits of agreement with confidence intervals are shown in Supplemental Table 2.

Discussion

In this prospective, multicenter study we found that ambrisentan and tadalafil combination therapy for a duration of 36 weeks significantly improved both RV and LV systolic and diastolic function, as analyzed by CMR-derived strain and SR in patients with SSc-PAH. We also demonstrated that the improvement of RV and LV strain and SR correlated with improvement in various clinical parameters such as the 6MWD, NT-proBNP, and hemodynamics, although there was no significant correlation between changes in RVEF and LVEF and these parameters. These findings may suggest that strain and SR, compared to RVEF and LVEF, may be more sensitive and reliable markers of clinical and hemodynamic improvement in response to PAH therapy, although such conclusion is guarded considering the relative small number of patients. Moreover, since calculation of RV and LV volumes requires time-consuming manual or semi-automated contouring of the RV and LV, the simple and fast strain and SR analysis, especially in RVFW by CMR, along with assessment of systolic and diastolic functions, offers a significant technical advantage.

Chronic pressure overload in PAH due to elevated PVR leads to RV hypertrophy, dilatation, and dysfunction. Longitudinal systolic strain measurement is well suited to assess RV function because RV contractility predominantly occurs in the longitudinal plane due to the principal orientation of myocardial fibers.[20,21] Previous reports have

Table 2. Changes in WHO FC, NT-proBNP, 6MWD, hemodynamics, and volumetric MRI parameters at 36 weeks of therapy compared to baseline.

Parameter	Baseline	Follow-up	Change	*P* value
WHO FC (I/II/III/IV)	0/8/13/0	1/11/9/0		
6MWD (m)	390 (260–438)	428 (311–468)	44 (–3 – 76)	0.003
NT-proBNP (pg/mL)	426 (140–1517)	329 (93–655)	–44 (–909 – 69)	0.053
RAP (mmHg)	6 (4–11)	5 (3–8)	–2 (–6 – 2)	0.11
mPAP (mmHg)	37 (33–46)	30 (24–36)	–9 (–12 – –6)	<0.0001
CI (L/min/m^2)	2.5 (2.2–3)	3.2 (2.6–3.8)	0.6 (–0.2 – 1.1)	0.0085
Stroke volume index (mL/m^2)	33 (28–42)	45 (37–54)	10 (1–16)	0.0005
PAWP (mmHg)	9 (6–12)	11 (8–14)	1 (–3 – 6)	0.25
PVR (Wood units)	6.8 (4–11)	3 (2–5.6)	–3.8 (–5.4 – 1.5)	< 0.0001
RVEF (%)	47 (42–54)	56 (53–64)	3 (–4 – 9)	< 0.0001
RVED volume (mL)	151 (139–172)	160 (129–166)	0 (–20 – 7)	0.65
RVES volume (mL)	80 (62–94)	58 (82–49)	–12 (–30 – –3)	0.003
RV mass (g)	28 (23–39)	28 (20–34)	–3 (–9 – 1)	0.06
LVEF (%)	64 (60–68)	63 (59–68)	1 (–6 – 4)	0.88
LVED volume (mL)	115 (91–137)	136 (119–161)	19 (11–40)	< 0.0001
LVES volume (mL)	39 (31–52)	50 (40–61)	7 (1–17)	0.004
LV mass (g)	88 (72–107)	97 (75–109)	7 (–6 – 14)	0.15

Data represent median (IQR) (n = 21 for each parameter).
6MWD, 6-min walk distance; NT-proBNP, N-Terminal pro-brain natriuretic peptide; mPAP, mean pulmonary arterial pressure; RAP, right atrial pressure; CI, cardiac index; PAWP, pulmonary arterial wedge pressure; PVR, pulmonary vascular resistance; RV, right ventricular; EF, ejection fraction; ED, endo diastolic; ES, endo systolic; LV, left ventricular; RVED, right ventricle end-diastolic; RVED vol, RVED volume; RVES, RV end-systolic volume; LVED vol, left ventricle end-diastolic volume; LVES vol, LV end-systolic volume.

Table 3. Changes in CMR RVFW strain parameters from baseline to 36 weeks.

Parameter	Baseline	Follow-up	Change	*P* value
pLS (%) (n = 21)	–20.5 (–24 – –13.9)	–26.4 (–30.5 – –24.8)	–5.2 (–11.2 – –3.6)	<0.0001
pLSRs (1/s) (n = 21)	–0.96 (–1.22 – –0.78)	–1.32 (–1.53 – –1.03)	–0.22 (–0.49 – –0.05)	< 0.0001
pLSRe (1/s) (n = 21)	0.77 (0.36–2.32)	1.0 (0.66–1.72)	0.35 (–0.35 – 0.58)	0.35
pLSRa (1/s) (n = 20)	0.79 (0.34–1.28)	1.52 (0.67–2.58)	0.48 (–0.28 – 1.22)	0.048
pCS (%) (n = 21)	–11.7 (–12.5 – –10.2)	–12.3 (–15.6 – –10.7)	–1.2 (–4.2 – 1.4)	0.09
pCSRs (1/s) (n = 21)	–0.49 (–0.58 – –0.43)	–0.49 (–0.83 – –0.44)	–0.01 (–0.17 – 0.08)	0.41
pCSRe (1/s) (n = 21)	0.48 (0.34–0.77)	0.77 (0.58–1.28)	0.29 (0.05–0.74)	0.0011
pCSRa (1/s) (n = 18)	0.37 (0.26–0.69)	0.29 (0.2–0.5)	–0.13 (–0.39 – 0.3)	0.17

Data expressed as median and IQR.
CMR, cardiac magnetic resonance; RVFW, right ventricular free wall; pLS, peak longitudinal strain; pLSRs, peak longitudinal systolic strain rate; pLSRe, peak longitudinal early diastolic strain rate; pLSRa, peak longitudinal atrial-diastolic strain rate; pCS, peak circumferential strain; pCSRs, peak circumferential systolic strain rate; pCSRe, peak circumferential atrial-diastolic strain rate.

demonstrated that decreased RV longitudinal strain in patients with pulmonary hypertension (PH) was correlated with disease severity[22,23] and mortality.[16,24] Moreover, Hardegree et al. demonstrated that, in response to therapy, patients with >5% improvement in RV free wall systolic strain had a greater than sevenfold lower mortality risk at four years.[25] Our results demonstrate that median improvement of RVFW pLS was 5.2% after combination therapy for 36 weeks. In addition, the improvement in RVFW pLS correlated with the improvement in 6MWD and mRAP which are well-known predictors of survival in PAH patients.[26] These results strongly suggest that ambrisentan and tadalafil combination therapy for SSc-PAH patients improves RV systolic function.

Our results do not demonstrate improvement in RV circumferential strain and SRs. A plausible explanation for this result is the fact that RV transverse motion in patients with PAH is associated with progressive RV failure[27] and RV

Table 4. Changes in CMR LV strain parameters from baseline to 36 weeks.

Parameter	Baseline	Follow-up	Change	*P* value
pLGS (%) (n = 18)	–19.1 (–22.4 – –14.7)	–20.9 (–23.6 – –18.4)	–0.9 (–8.0 – 0.5)	0.039
pLGSRs (1/s) (n = 18)	–0.94 (–1.17 – –0.81)	–1.0 (–1.2 – –0.88)	–0.08 (–0.39 – 0.07)	0.268
pLGSRe (1/s) (n = 18)	0.9 (0.36–1.38)	1.48 (0.99–2.25)	0.62 (0.17–1.27)	0.0017
pLGSRa (1/s) (n = 18)	0.74 (0.4–1.49)	0.43 (0.31–0.68)	–0.08 (–1.16 – 0.06)	0.035
pCS (%) (n = 21)	–18.1 (–21.5 – –16.1)	–20.6 (–23.2 – –18.4)	–0.7 (–3.4 – 0.8)	0.103
pCSRs (1/s) (n = 21)	–0.97 (–1.17 – –0.8)	–0.95 (–1.22 – –0.83)	0.0 (–0.21 – 1.05)	0.712
pCSRe (1/s) (n = 20)	0.91 (0.75–1.38)	1.23 (0.71–1.46)	0.01 (–0.1 – 0.52)	0.225
pCSRa (1/s) (n = 19)	0.53 (0.36–0.93)	0.51 (0.41–0.68)	–0.05 (–0.27 – 0.06)	0.411

Data expressed as median and interquartile range.
CMR, cardiac magnetic resonance; LV, left ventricular; pGLS, peak global longitudinal strain; pGLSRs, peak global longitudinal systolic strain rate; pGLSRe, peak global longitudinal early diastolic strain rate; pGLSRa, peak global longitudinal atrial-diastolic strain rate; pCS, peak circumferential strain; pCSRs, peak circumferential systolic strain rate; pCSRe, peak circumferential atrial-diastolic strain rate.

Table 5. Changes in LV longitudinal IVS and LW strain and SR, and LV circumferential IVS and FW strain and SR from baseline to 36 weeks.

Parameter	Baseline	Follow-up	Change	*P* value
IVS pLS (%)	–14.4 (–10.8 – –16.6)	–16.6 (–12.5 – –19.8)	–1.0 (–5.9 – 0.5)	0.027
IVS pLSRs (1/s)	–0.67 (–0.88 – –0.6)	–0.74 (–0.95 – –0.63)	–0.08 (–0.2 – –0.06)	0.181
IVS pLSRe (1/s)	0.89 (0.35–1.33)	1.31 (0.92–1.82)	0.21 (–0.12 – 1.04)	0.02
IVS pLSRa (1/s) (n = 17)	0.61 (0.25–0.9)	0.29 (0.2–0.53)	–0.05 (–0.48 – 0.13)	0.495
LW pLS (%)	–22.6 (–27.7 – –16.7)	–24.4 (–31.3 – –21.5)	–3.1 (–9.0 – 0.56)	0.089
LW pLSRa (1/s) (n = 18)	–1.08 (–1.36 – –0.94)	–1.19 (–1.56 – –0.98)	–0.07 (–0.51 – 0.11)	0.17
LW pLSRe (1/s)	0.94 (0.51–1.97)	1.85 (1.45–3.32)	0.73 (–0.59 – 1.63)	0.02
LW pLSRa (1/s)	0.89 (0.45–1.6)	0.42 (0.26–0.68)	–0.22 (–1.43 – 0.11)	0.03
IVS pCS (%)	–18.8 (–22.5 – –16.3)	–20.7 (–23.9 – –17.7)	–1.07 (–4.53 – 1.02)	0.2
IVS pCSRs (1/s)	–0.97 (–1.24 – –0.82)	–0.95 (–1.28 – –0.8)	0.02 (–0.15 – 0.2)	0.7
IVS pCSRe (1/s) (n = 20)	0.98 (0.52–1.39)	1.22 (0.88–1.54)	0.06 (–0.17 – 0.45)	0.02
IVS pCSRa (1/s) (n = 19)	0.56 (0.37–0.93)	0.47 (0.35–0.66)	–0.12 (–0.42 – 0.05)	0.106
FW pCS (%)	–18 (–21.1 – –16)	–20.2 (–23.7 – –17.8)	–1.15 (–3.95 – 1.76)	0.164
FW pCSRs (1/s)	–0.95 (–1.18 – –0.79)	–0.95 (–1.29 – –0.82)	–0.02 (–0.29 – 0.18)	0.511
FW pCSRe (1/s) (n = 20)	1.0 (0.75–1.29)	1.17 (0.81–1.7)	0.01 (–0.16 – 0.49)	0.436
FW pCSRa (1/s) (n = 19)	0.51 (0.38–0.9)	0.57 (0.39–0.63)	–0.01 (–0.18 – 0.08)	0.76

Data expressed as median and IQR.
LV, left ventricular; SR, strain rate; IVS, interventricular septum; LW, lateral wall; FW, free wall; pLS, peak longitudinal strain; pLSRs, peak longitudinal systolic strain rate; pLSRe, peak longitudinal early diastolic strain rate; pLSRa, peak longitudinal atrial-diastolic strain rate; pCS, peak circumferential strain; pCSRs, peak circumferential systolic strain rate; pCSRe, peak circumferential atrial-diastolic strain rate.

function of our patients was relatively preserved (median RVEF was 47%).

A previous report demonstrated a correlation between RVEF, and RV strain parameters,[15] NT-proBNP,[28] and PVR[29] in contrast with our results which fail to demonstrate such correlation. We believe this is most likely related to the relatively small number of patients in our study. In fact, there was a trend between improved RVEF and a drop in NT-proBNP ($\rho = -0.38$, $P = 0.10$) and PVR ($\rho = -0.43$, $P = 0.0778$) and improved RV SV index ($\rho = 0.39$, $P = 0.0842$). Another potential reason for a lack of correlation is the fairly preserved baseline RVEF in our study (median RVEF of 47%). As for the left heart disease, while it is well-known that patients with impaired LVEF have a high risk of all-cause mortality, this effect is less apparent in patients with LVEF > 45%.[30] The inherent insensitivity of EF might limit its ability to identify degree of LV systolic impairment, which may apply to patients with right heart failure related to PAH.

Interestingly, the improvement in RVFW pLSRa correlated with a reduction in mRAP, mPAP, and PVR measurements. RV SRa is determined by RV compliance and RA

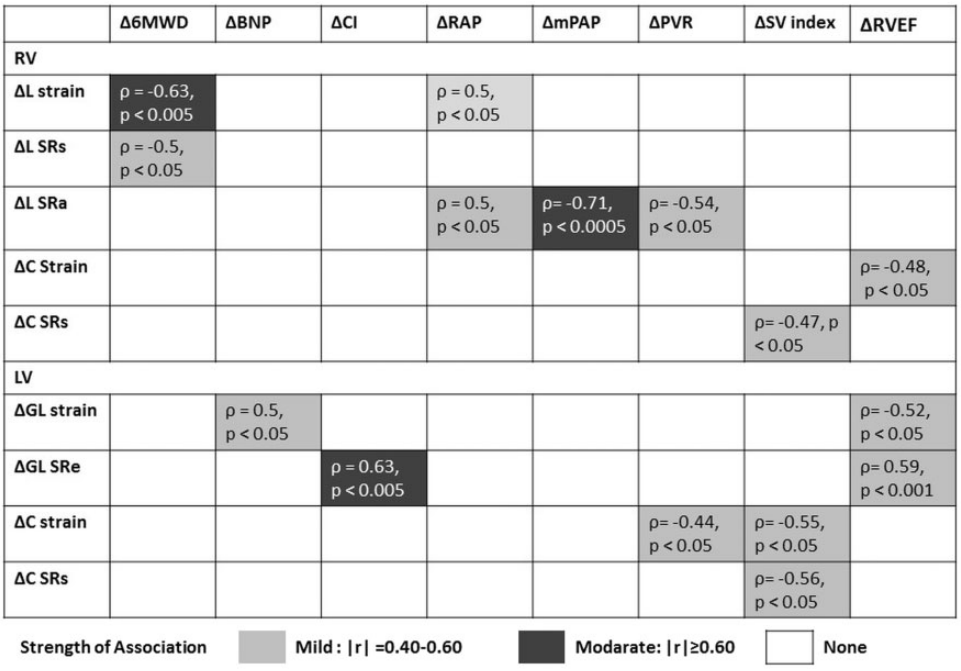

Fig. 3. Correlations between clinical parameters and CMR-derived peak systolic strain and peak SR parameters. Correlation between changes in 6MWD, NT-proBNP, and hemodynamic parameters, and CMR-derived strain and SR parameters from baseline to 36 weeks. 6MWD, 6-min walk distance; NT-proBNP, N Terminal pro-brain natriuretic peptide; CI, cardiac index; RAP, right atrial pressure; mPAP, mean pulmonary arterial pressure; PVR, pulmonary vascular resistance; SV, stroke volume; RV, right ventricular; LV, left ventricular; EF, ejection fraction; L, longitudinal; C, circumferential; GL, global; SRs, peak systolic strain rate; SRe, peak early diastolic strain rate; SRa, peak atrial-diastolic strain rate.

contraction during cardiac cycle. Okumura et al. demonstrated that there was moderate correlation between RV SRa derived from echocardiography and tau which is the gold standard for evaluation of diastolic function derived from high-fidelity micromanometer catheter.[31] Based on these findings, the increase in RV SRa suggests improvement in RV diastolic function in response to combination therapy in SSc-PAH patients. The most likely explanation for the improvement in RV diastolic function is the significant reduction in RV afterload provided by combination therapy. Another possibility that cannot be ruled out at this time is a direct effect of PAH drugs on cardiomyocyte function. PDE 5 is present in the human myocardium and the PDE 5 inhibitor sildenafil has been shown to reverse hypertrophy and improve cardiomyocyte contractile function in animal models.[32,33]

LV dysfunction in PAH is closely related to changes in RV function, either via direct interventricular dependence, which in PAH patients leads to limitations in LV diastolic filling by leftward septum bowing or via hemodynamic effects as a result of a decrease in RV output. In our study, although there was no significant change in LVEF before and after treatment, we saw increased LVEDV and LVESV, suggesting improved LV filling, as well as significant improvements in LV pGLS and pGLSRe. Actually, an increase in LVEDV was significantly correlated with improvement in LV pGLSRe ($\rho = 0.74$, $P = 0.0004$) and a there was a trend for inverse correlation with LV pGLS ($\rho = -0.43$, $P = 0.0778$). The improvement of LV function has particular importance in patients with SSc-PAH, because LV involvement is a known complication of SSc patients associated with increased mortality.[12,34] The change in LV pGLSRe also correlated with changes in CI. These results underline the importance of changes in LV systolic and diastolic function in response to therapy in PAH. In addition, changes in LV pCS, LV pCSRs, and RV FW pCSRs correlated with SV index which has been established as a strong predictor of mortality in patients with SSc-PAH.[6] A previous study reported that LV circumferential strain had a relatively greater contribution to the SV than longitudinal strain in patients with hypertrophic cardiac disease.[35] These results suggest that both LV and RV circumferential systolic strain parameters are more related to SV than LV and RV longitudinal systolic strain parameters in two distinct cardiac diseases.

Our results indicate that LV longitudinal strain and SR were significantly improved although there was no significant change in LV circumferential strain and SR. In some left heart diseases where longitudinal function is significantly impaired, circumferential function can to a certain extent compensate for the initial reduction in longitudinal function, with both LVEF and fractional shortening often being above normal.[17] Burkett et al. demonstrated that there was a generally smaller reduction in LV circumferential strain compared to longitudinal strain in children with PAH compared with control individuals. Taken together

with our results, this suggests that leftward septal shift or interventricular dependence in PAH affect contraction of longitudinal fibers more than circumferential fibers. In keeping with our results of regional analysis comparing LV IVS with non-LV IVS, the improvement in LV IVS strain and SR contributes more to the improvement in the global LV function.

Our results showed that changes in LV pGLS were 0.9%. In light of the report by Sengelov et al. showing that a 1% reduction of LV pGLS in patients with heart failure with reduced EF was associated with increased mortality: hazard ratio = 1.15 (95% confidence interval [CI] = 1.04–1.27, $P = 0.008$),[36] a 0.9% improvement of LV pGLS in patients with SSc-PAH may be significant in terms of improving survival.

Most importantly, taken together the results of this study suggest that RV and LV strain and SR respond to treatment in SSc-PAH.

Most strain and SR measurements in patients with PH have been performed using echocardiographic studies.[16,23,24,37] Echocardiography is a convenient and repeatedly accessible tool although the complex RV chamber geometry limits accurate assessment of RV function. In contrast, MRI allows for observer-independent evaluation of RV morphology and function and is considered the gold standard for these assessments,[8,38,39] although it requires a dedicated program and expertise, limiting its widespread use. Nevertheless, the present results of strain and SR derived from CMR with MTT software may be more accurate and reliable than results reported in previous studies.[14] Indeed, our reproducibility data demonstrated low limits of agreement.

Limitations

There are several limitations to the present study. A single software system was used in the analysis of image obtained in clinical practice on four different MRI systems and two different sequences. This may affect the absolute value of the strain and SR,[40,41] although the effect is likely smaller when comparisons are made before and after treatment. This was necessary due to the multicenter nature of the current study; however, because all patients were scanned on the same type of scanner with the same protocol pre- and post-therapy, these differences will be minimized.

Our study is limited by the small number of patients and by the lack of a placebo group for comparison. However, there was uniform improvement in functional, hemodynamic, serum, and imaging biomarkers in our cohort as previously reported,[13] which support the validity of effective measurable changes in the imaging parameters discussed herein.

All of our patients had WHO FC II or III symptom at the time of baseline evaluation. Thus, the utility of RV and LV strain and SR measures in assessment of more severe disease may not apply.

Although our results showed that combination therapy was associated with significant improvements in LV systolic function, reflected by increased LV pGLS, this result should be considered with caution considering the small change in LV pLGS relative to the large 95% CI by Bland–Altman analysis.

This study is the first study to assess the impact of ambrisentan and tadalafil combination therapy on LV and RV myocardial systolic and diastolic function as assessed by CMR with MTT in the context of a multicenter trial. In this study, combination therapy was associated with significant improvement in RV and LV longitudinal systolic and diastolic parameters. The improvement in RV and LV strain and SR were related to improvements in 6MWD, NT-proBNP, and hemodynamics parameters, all established prognostic markers in PAH.

Acknowledgments

The work was supported by a fellowship grant from the Uehara Memorial Foundation, the Mochida Memorial Foundation for Medical and Pharmaceutical Research, the Ito Foundation for the Promotion of Medical Science, and the Japanese Society for the Promotion of Science.

Declaration of conflicting interests

The author(s) declare that there is no conflict of interest.

Funding

Work supported by The National Institutes of Health/National Heart, Lung, and Blood Institute awards P50 HL084946 (PMH), HL114910 (PMH), and K23HL90038491 (SCM). Gilead Inc. and United Therapeutics Inc. provided all the drugs (ambrisentan and tadalafil, respectively) free of charge for the entire duration of the study (36 weeks) and for one year after completion of the study. They had no role in the design or monitoring of the study, acquisition of clinical or imaging data, statistical analysis, interpretation of the results, and writing of the manuscript.

References

1. Steen VD and Medsger TA. Changes in causes of death in systemic sclerosis, 1972-2002. *Ann Rheum Dis* 2007; 66: 940–944.
2. Galie N, Ghofrani HA, Torbicki A, et al. Sildenafil citrate therapy for pulmonary arterial hypertension. *N Engl J Med* 2005; 353: 2148–2157.
3. Galie N, Olschewski H, Oudiz RJ, et al. Ambrisentan for the treatment of pulmonary arterial hypertension: Results of the ambrisentan in pulmonary arterial hypertension, randomized, double-blind, placebo-controlled, multicenter, efficacy (aries) study 1 and 2. *Circulation* 2008; 117: 3010–3019.
4. Vonk-Noordegraaf A, Haddad F, Chin KM, et al. Right heart adaptation to pulmonary arterial hypertension: Physiology and pathobiology. *J Am Coll Cardiol* 2013; 62: D22–33.
5. Mathai SC, Sibley CT, Forfia PR, et al. Tricuspid annular plane systolic excursion is a robust outcome measure in systemic sclerosis-associated pulmonary arterial hypertension. *J Rheumatol* 2011; 38: 2410–2418.
6. Campo A, Mathai SC, Le Pavec J, et al. Hemodynamic predictors of survival in scleroderma-related pulmonary arterial hypertension. *Am J Respir Crit Care Med* 2010; 182: 252–260.

7. Forfia PR, Fisher MR, Mathai SC, et al. Tricuspid annular displacement predicts survival in pulmonary hypertension. *Am J Respir Crit Care Med* 2006; 174: 1034–1041.
8. van de Veerdonk MC, Kind T, Marcus JT, et al. Progressive right ventricular dysfunction in patients with pulmonary arterial hypertension responding to therapy. *J Am Coll Cardiol* 2011; 58: 2511–2519.
9. Damiano RJ Jr, La Follette P Jr, Cox JL, et al. Significant left ventricular contribution to right ventricular systolic function. *Am J Physiol* 1991; 261: H1514–1524.
10. Tonelli AR, Plana JC, Heresi GA, et al. Prevalence and prognostic value of left ventricular diastolic dysfunction in idiopathic and heritable pulmonary arterial hypertension. *Chest* 2012; 141: 1457–1465.
11. Burkett DA, Slorach C, Patel SS, et al. Left ventricular myocardial function in children with pulmonary hypertension: Relation to right ventricular performance and hemodynamics. *Circ Cardiovasc Imaging* 2015; 8: e003260.
12. Hardegree EL, Sachdev A, Fenstad ER, et al. Impaired left ventricular mechanics in pulmonary arterial hypertension: Identification of a cohort at high risk. *Circ Heart Fail* 2013; 6: 748–755.
13. Hassoun PM, Zamanian RT, Damico R, et al. Ambrisentan and tadalafil up-front combination therapy in scleroderma-associated pulmonary arterial hypertension. *Am J Respir Crit Care Med* 2015; 192: 1102–1110.
14. Ohyama Y, Ambale-Venkatesh B, Chamera E, et al. Comparison of strain measurement from multimodality tissue tracking with strain-encoding mri and harmonic phase mri in pulmonary hypertension. *Int J Cardiol* 2015; 182: 342–348.
15. Oyama-Manabe N, Sato T, Tsujino I, et al. The strain-encoded (senc) mr imaging for detection of global right ventricular dysfunction in pulmonary hypertension. *Int J Cardiovasc Imaging* 2012; 29: 371–378.
16. Fine NM, Chen L, Bastiansen PM, et al. Outcome prediction by quantitative right ventricular function assessment in 575 subjects evaluated for pulmonary hypertension. *Circ Cardiovasc Imaging* 2013; 6: 711–721.
17. Cikes M and Solomon SD. Beyond ejection fraction: An integrative approach for assessment of cardiac structure and function in heart failure. *Eur Heart J* 2016; 37: 1642–1650.
18. Zareian M, Ciuffo L, Habibi M, et al. Left atrial structure and functional quantitation using cardiovascular magnetic resonance and multimodality tissue tracking: Validation and reproducibility assessment. *J Cardiovasc Magn Reson* 2015; 17: 52.
19. Imai M, Ambale Venkatesh B, Samiei S, et al. Multi-ethnic study of atherosclerosis: Association between left atrial function using tissue tracking from cine mr imaging and myocardial fibrosis. *Radiology* 2014; 273: 703–713.
20. Leather HA, Ama R, Missant C, et al. Longitudinal but not circumferential deformation reflects global contractile function in the right ventricle with open pericardium. *Am J Physiol Heart Circ Physiol* 2006; 290: H2369–2375.
21. Rushmer RF, Crystal DK and Wagner C. The functional anatomy of ventricular contraction. *Circ Res* 1953; 1: 162–170.
22. Marwick TH. Measurement of strain and strain rate by echocardiography: Ready for prime time? *J Am Coll Cardiol* 2006; 47: 1313–1327.
23. Puwanant S, Park M, Popovic ZB, et al. Ventricular geometry, strain, and rotational mechanics in pulmonary hypertension. *Circulation* 2010; 121: 259–266.
24. Sachdev A, Villarraga HR, Frantz RP, et al. Right ventricular strain for prediction of survival in patients with pulmonary arterial hypertension. *Chest* 2011; 139: 1299–1309.
25. Hardegree EL, Sachdev A, Villarraga HR, et al. Role of serial quantitative assessment of right ventricular function by strain in pulmonary arterial hypertension. *Am J Cardiol* 2013; 111: 143–148.
26. McLaughlin VV, Gaine SP, Howard LS, et al. Treatment goals of pulmonary hypertension. *J Am Coll Cardiol* 2013; 62: D73–81.
27. Mauritz GJ, Kind T, Marcus JT, et al. Progressive changes in right ventricular geometric shortening and long-term survival in pulmonary arterial hypertension. *Chest* 2012; 141: 935–943.
28. Blyth KG, Groenning BA, Mark PB, et al. Nt-probnp can be used to detect right ventricular systolic dysfunction in pulmonary hypertension. *Eur Respir J* 2007; 29: 737–744.
29. Querejeta Roca G, Campbell P, Claggett B, et al. Impact of lowering pulmonary vascular resistance on right and left ventricular deformation in pulmonary arterial hypertension. *Eur J Heart Fail* 2015; 17: 63–73.
30. Curtis JP, Sokol SI, Wang Y, et al. The association of left ventricular ejection fraction, mortality, and cause of death in stable outpatients with heart failure. *J Am Coll Cardiol* 2003; 42: 736–742.
31. Okumura K, Slorach C, Mroczek D, et al. Right ventricular diastolic performance in children with pulmonary arterial hypertension associated with congenital heart disease: Correlation of echocardiographic parameters with invasive reference standards by high-fidelity micromanometer catheter. *Circ Cardiovasc Imaging* 2014; 7: 491–501.
32. Borlaug BA, Melenovsky V, Marhin T, et al. Sildenafil inhibits beta-adrenergic-stimulated cardiac contractility in humans. *Circulation* 2005; 112: 2642–2649.
33. Takimoto E, Champion HC, Li M, et al. Chronic inhibition of cyclic gmp phosphodiesterase 5a prevents and reverses cardiac hypertrophy. *Nat Med* 2005; 11: 214–222.
34. Steen VD and Medsger TA Jr. Severe organ involvement in systemic sclerosis with diffuse scleroderma. *Arthritis Rheum* 2000; 43: 2437–2444.
35. Maciver DH. The relative impact of circumferential and longitudinal shortening on left ventricular ejection fraction and stroke volume. *Exp Clin Cardiol* 2012; 17: 5–11.
36. Sengelov M, Jorgensen PG, Jensen JS, et al. Global longitudinal strain is a superior predictor of all-cause mortality in heart failure with reduced ejection fraction. *JACC Cardiovasc Imaging* 2015; 8: 1351–1359.
37. Pirat B, McCulloch ML and Zoghbi WA. Evaluation of global and regional right ventricular systolic function in patients with pulmonary hypertension using a novel speckle tracking method. *Am J Cardiol* 2006; 98: 699–704.
38. Grothues F, Moon JC, Bellenger NG, et al. Interstudy reproducibility of right ventricular volumes, function, and mass with

cardiovascular magnetic resonance. *Am Heart J* 2004; 147: 218–223.
39. Alfakih K, Reid S, Jones T, et al. Assessment of ventricular function and mass by cardiac magnetic resonance imaging. *Eur Radiol* 2004; 14: 1813–1822.
40. Pedrizzetti G, Claus P, Kilner PJ, et al. Principles of cardiovascular magnetic resonance feature tracking and echocardiographic speckle tracking for informed clinical use. *J Cardiovasc Magn Reson* 2016; 18: 51.
41. Schuster A, Hor KN, Kowallick JT, et al. Cardiovascular magnetic resonance myocardial feature tracking: Concepts and clinical applications. *Circ Cardiovasc Imaging* 2016; 9: e004077.